



FEA Information

Information for the LS-DYNA Global Community

www.feainformation.com

Second Issue, November 2000

Welcome to the second issue of our newsletter. Our goal is to bring you a monthly synopsis of the additions/revisions to the FEA Information web sites and to assist you in focusing your attention to new material when you consult our web pages on return visits.

When available, we will print technical information on Livermore Software Technology Corporation's LS-DYNA and information from our commercial participants.

If you know someone that would like the News, please have them e-mail me their address:
Marsha – mv@feainformation.com

| Page | Article | Author |
|-------------|---|------------------------------------|
| 1- 13 | Version 960 Overview | Livermore Software Technology Corp |
| 14 | Implicit FAQ | Dr. Bradley Maker |
| 15 | Virtual Proving Ground | Bruce Morse & Arthur Tang |
| 16 | FEA Site Summary Recommended Resource Site | Marsha Victory |
| 17 | Publications | Denette Trowbridge |
| 18 | November Sponsors | LSTC ETA OASYS |

LS-DYNA VERSION 960 OVERVIEW

NEW CONSTITUTIVE MODELS

***MAT_WINFRITH_CONCRETE**

The Winfrith concrete model is a smeared crack (sometimes known as pseudo crack), smeared rebar model, implemented in the 8-node single integration point continuum element. This model was developed by Broadhouse [1995] over many years and has been validated against experiments. The Fortran subroutines and quality assurance test problems were also provided to LSTC by the Winfrith Technology Center. The rebar is defined by the keyword: *MAT_WINFRITH_CONCRETE_REINFORCEMENT which follows.

The Winfrith concrete model generates an additional binary output file containing information on crack locations, directions, and widths.

***MAT_WINFRITH_CONCRETE_REINFORCEMENT**

Reinforcement may be defined in specific groups of elements, but it is usually more convenient to define a two-dimensional mat in a specified layer of a specified material. Reinforcement quantity is defined as the ratio of the cross-sectional area of steel relative to the cross-sectional area of concrete in the element (or layer).

***MAT_SOFT_TISSUE_VISCO**

This material is a transversely isotropic hyperelastic model for representing biological soft tissues such as ligaments, tendons, and fascia. The representation provides an isotropic Mooney-Rivlin matrix reinforced by fibers having a strain energy contribution with the qualitative material behavior of collagen. The model has a viscoelasticity option, which activates a six-term Prony series kernel for the relaxation function. In this case, the hyperelastic strain energy represents the elastic (long-time) response. See Weiss et al. [1996] and Puso and Weiss [1998] for additional details. The material is available for use with brick and shell elements. When used with shell elements, the Belytschko-Tsay formulation (#2) must be selected.

The overall strain energy W is "uncoupled" and includes two isotropic deviatoric matrix terms, a fiber term F , and a bulk term:

$$W = C_1 \left(\tilde{I}_1 - 3 \right) + C_2 \left(\tilde{I}_2 - 3 \right) + F(\lambda) + \frac{1}{2} K [\ln(J)]^2$$

Here, \tilde{I}_1 and \tilde{I}_2 are the deviatoric invariants of the right Cauchy deformation tensor, λ is the deviatoric part of the stretch along the current fiber direction, and $J = \det \mathbf{F}$ is the volume ratio. The material coefficients C_1 and C_2 are the Mooney-Rivlin coefficients, while K is the effective bulk modulus.

The derivatives of the fiber term F are defined to capture the behavior of crimped collagen. The fibers are assumed to be unable to resist compressive loading; thus, the model is isotropic when $\lambda < 1$. An exponential function describes the straightening of the fibers, while a linear function describes the behavior of the fibers once they are straightened past a critical fiber stretch level $\lambda \geq \lambda^*$.

$$\frac{\partial F}{\partial \lambda} = \left\{ \begin{array}{ll} 0 & \lambda < 1 \\ \frac{C_3}{\lambda} [\exp(C_4(\lambda - 1)) - 1] & \lambda < \lambda^* \\ \frac{1}{\lambda} (C_5\lambda + C_6) & \lambda \geq \lambda^* \end{array} \right\}$$

Coefficients C_3 , C_4 , and C_5 must be defined by the user. C_6 is determined by LS-DYNA to ensure stress continuity at $\lambda = \lambda^*$. Sample values for the material coefficients $C_1 - C_5$ and λ^* for ligament tissue can be found in Quapp and Weiss [1998]. The bulk modulus K should be at least 3 orders of magnitude larger than C_1 to ensure near-incompressible material behavior.

Viscoelasticity is included by a convolution integral representation for the time-dependent second Piola-Kirchhoff stress $S(C, t)$:

$$S(C, t) = S^e(C) + \int_0^t 2G(t-s) \frac{\partial W}{\partial C(s)} ds$$

Here, S^e is the elastic part of the second PK stress as derived from the strain energy, and $G(t-s)$ is the reduced relaxation function, represented by a Prony series:

$$G(t) = \sum_{i=1}^6 S_i \exp\left(-\frac{t}{T_i}\right).$$

***MAT_SIMPLIFIED_JOHNSON_COOK**

The Johnson/Cook strain rate sensitive plasticity is used for problems where the strain rates vary over a large range. In this simplified model, thermal effects and damage are ignored, and the maximum stress is directly limited since thermal softening which is very significant in reducing the yield stress under adiabatic loading is not available. An iterative plane stress update is used for the shell elements, but due to the simplifications related to thermal softening and damage, this model is 50% faster than the full Johnson/Cook implementation. To compensate for the lack of thermal softening, limiting stress values are used to keep the stresses within reasonable limits. A resultant formulation for the Belytschko-Tsay, the C0 Triangle, and the fully integrated type 16 shell elements is activated by specifying either zero or one through thickness integration point on the *SHELL_SECTION card. This latter option is less accurate than through thickness integration but is somewhat faster. Since the stresses are not computed in the resultant formulation, the stress output to the databases for the resultant elements are zero. This model is also available for the Hughes-Liu beam, the Belytschko-Schwer beam, and the truss element. For the resultant beam formulation, the rate effects are approximated by the axial rate since the thickness of the beam about its bending axes is unknown. The linear bulk modulus rather than an equation-of-state is used to determine the pressure, since the primary use of this model is for structural analysis.

Johnson and Cook express the flow stress as

$$\sigma_y = \left(A + B \bar{\epsilon}^n \right) (1 + c \ln \dot{\epsilon}^*)$$

where

A, B, C and n are input constants

$\bar{\epsilon}^p$ effective plastic strain

$$\dot{\epsilon}^* = \frac{\dot{\bar{\epsilon}}}{\dot{\epsilon}_0} \text{ effective strain rate for } \dot{\epsilon}_0 = 1s^{-1}$$

The maximum stress is limited by *sigmax* and *sigsat* by:

$$\sigma_y = \min \left\{ \min \left[A + B\bar{\epsilon}^n, \text{sigmax} \right] (1 + c \ln \dot{\epsilon}^*), \text{sigsat} \right\}$$

Failure occurs when the effective plastic strain exceeds a user-defined value.

***MAT_SPOTWELD_DAMAGE**

This material model applies to beam element type 9 for spot welds. In version 960 a damage option has been added to model the gradual reduction of force that is seen experimentally when spot-welds fail. These beam elements, based on the Hughes-Liu beam formulation, may be placed between any two deformable shell surfaces and tied with constraint contact, *CONTACT_SPOTWELD, which eliminates the need to have adjacent nodes at spot weld locations. Beam spot welds may be placed between rigid bodies and rigid/deformable bodies by making the node on one end of the spot weld a rigid body node which can be an extra node for the rigid body, see *CONSTRAINED_EXTRA_NODES_OPTION. In the same way rigid bodies may also be tied together with this spot weld option. This weld option should not be used with rigid body switching. In flat topologies the shell elements have an unconstrained drilling degree-of-freedom which prevents torsional forces from being transmitted.

Beam force resultants for MAT_SPOTWELD are written to the spot weld force file, SWFORC, and the file for element stresses and resultants for designated elements, ELOUT.

The weld material is modeled with isotropic hardening plasticity coupled to two failure models. The first model specifies a failure strain, which fails each integration point in the spot weld independently. The second model fails the entire weld if the resultants are outside of the failure surface defined by:

$$\left(\frac{\max(N_{rr}, 0)}{N_{rrF}} \right)^2 + \left(\frac{N_{rs}}{N_{rsF}} \right)^2 + \left(\frac{N_{rt}}{N_{rtF}} \right)^2 + \left(\frac{M_{rr}}{M_{rrF}} \right)^2 + \left(\frac{M_{ss}}{M_{ssF}} \right)^2 + \left(\frac{M_{tt}}{M_{ttF}} \right)^2 - 1 = 0$$

where the *numerators* in the equation are the resultants calculated in the local coordinates of the cross section, and the **denominators** are the values specified in the input

If the failure strain is set to zero, the failure strain model is not used. In a similar manner, when the value of a resultant at failure is set to zero, the corresponding term in the failure surface is ignored. For example, if only N_{rrF} is nonzero, the failure surface is reduced to $|N_{rr}| = N_{rrF}$. None, either, or both of the failure models may be active depending on the specified input values.

The inertias of the spot welds are scaled during the first time step so that their stable time step size is Δt . A strong compressive load on the spot weld at a later time may reduce the length of the spot weld so that stable time step size drops below Δt . If the value of Δt is zero, mass scaling is not performed, and the spot welds will probably limit the time step size. Under most circumstances, the inertias of the spot welds are small enough that scaling them will have a negligible effect on the structural response and the use of this option is encouraged.

Spot-weld force history data is written into the SWFORC ASCII file. In this database the resultant moments are not available, but they are in the binary time history database.

The constitutive properties for the damaged material are obtained from the undamaged material properties. The amount of damage evolved is represented by the constant, ω , which varies from zero if no damage has occurred to unity for complete rupture. For uniaxial loading, the nominal stress in the damaged material is given by

$$\sigma_{nominal} = \frac{P}{A}$$

where P is the applied load and A is the surface area. The true stress is given by:

$$\sigma_{true} = \frac{P}{A - A_{loss}}$$

where A_{loss} is the void area. The damage variable can then be defined:

$$\omega = \frac{A_{loss}}{A} \quad 0 \leq \omega \leq 1$$

In this model damage is defined in terms of plastic strain after the failure strain is exceeded:

$$\omega = \frac{\epsilon_{eff}^p - \epsilon_{failure}^p}{\epsilon_{rupture}^p - \epsilon_{failure}^p} \quad \text{if} \quad \epsilon_{failure}^p \leq \epsilon_{eff}^p \leq \epsilon_{rupture}^p$$

After exceeding the failure strain softening begins and continues until the rupture strain is reached.

***MAT_ELASTIC_VISCOPLASTIC_THERMAL**

This is an elastic viscoplastic material with thermal effects. The uniaxial stress-strain curve has the form:

$$\begin{aligned} \sigma(\epsilon_{eff}^p, \dot{\epsilon}_{eff}^p) = & \sigma_0 + Q_{r1}(1 - \exp(-C_{r1}\epsilon_{eff}^p)) + Q_{r2}(1 - \exp(-C_{r2}\epsilon_{eff}^p)) \\ & + Q_{\chi1}(1 - \exp(-C_{\chi1}\epsilon_{eff}^p)) + Q_{\chi2}(1 - \exp(-C_{\chi2}\epsilon_{eff}^p)) \\ & + V_k \dot{\epsilon}_{eff}^p V_m \end{aligned}$$

Young's modulus, Poisson's ratio, and the coefficient of thermal expansion can be optionally defined as a function of temperature, and the inelastic stress-strain equation can be scaled by a constant, which also varies with temperature. These variations are defined by using load curves

***MAT_FINITE_ELASTIC_STRAIN_PLASTICITY**

An elasto-plastic material with an arbitrary stress versus strain curve and arbitrary strain rate dependency can be defined. The elastic response of this model uses a finite strain formulation so that large elastic strains can develop before yielding occurs. This model is available for solid elements only.

The stress strain behavior may be treated by a bilinear stress strain curve by defining the tangent modulus, or by defining an effective stress versus effective plastic strain curve. The most general approach is to use the table where the stress versus strain curves are defined as a function of strain rate.

Three options to account for strain rate effects are possible.

I. Strain rate may be accounted for using the Cowper and Symonds model, which scales the yield stress with the factor

$$1 + \left(\frac{\dot{\epsilon}}{C} \right)^{1/p}$$

where $\dot{\epsilon}$ is the strain rate. $\dot{\epsilon} = \sqrt{\dot{\epsilon}_{ij} \dot{\epsilon}_{ij}}$.

II. For complete generality a load curve to scale the yield stress may be input instead. In this curve the scale factor versus strain rate is defined.

III. If different stress versus strain curves can be provided for various strain rates, the option using the reference to a table can be used.

***MAT_LAYERED_LINEAR_PLASTICITY**

A layered elastoplastic material with an arbitrary stress versus strain curve and an arbitrary strain rate dependency can be defined. This material must be used with the user defined integration rules, see *INTEGRATION-SHELL, for modeling laminated composite and sandwich shells where each layer can be represented by elastoplastic behavior with constitutive constants that vary from layer to layer. Lamination theory is applied to correct for the assumption of a uniform constant shear strain through the thickness of the shell. Unless this correction is applied, the stiffness of the shell can be grossly incorrect leading to poor results. Generally, without the correction the results are too stiff.. This model is available for shell elements only.

The stress strain behavior can be defined by a load curve, and three options are available to account for strain rate effects:

I. Strain rate may be accounted for using the Cowper and Symonds model, which scales the yield stress with the factor

$$1 + \left(\frac{\dot{\epsilon}}{C} \right)^{1/p}$$

where $\dot{\epsilon}$ is the strain rate. $\dot{\epsilon} = \sqrt{\dot{\epsilon}_{ij} \dot{\epsilon}_{ij}}$.

II. For complete generality a load curve (LCSR) to scale the yield stress may be input instead. In this curve the scale factor versus strain rate is defined.

III. If different stress versus strain curves can be provided for various strain rates, the option using the reference to a table can be used. Then the table input in *DEFINE_TABLE has to be used.

*MAT_UNIFIED_CREEP

This is an elastic creep model for modeling creep behavior when plastic behavior is not considered. In this model the effective creep strain, $\bar{\epsilon}^c$, given as:

$$\bar{\epsilon}^c = A\bar{\sigma}^n \bar{t}^m$$

where A , n , and m are constants and \bar{t} is the effective time. The effective stress, $\bar{\sigma}$, is defined as:

$$\bar{\sigma} = \sqrt{\frac{3}{2} \sigma_{ij} \sigma_{ij}}$$

The creep strain, therefore, is only a function of the deviatoric stresses. The volumetric behavior for this material is assumed to be elastic. By varying the time constant m , primary creep ($m < 1$), secondary creep ($m = 1$), and tertiary creep ($m > 1$) can be modeled. The description of this model is available, Whirley and Henshall (1992).

*MAT_COMPOSITE_LAYUP

This material is for modeling the elastic responses of composite lay-ups that have an arbitrary number of layers through the shell thickness. A pre-integration is used to compute the extensional, bending, and coupling stiffness for use with the Belytschko-Tsay resultant shell formulation. The angles of the local material axes are specified from layer to layer in the *SECTION_SHELL input. This material model must be used with the user defined integration rule for shells, which allows the elastic constants to change from integration point to integration point. Since the stresses are not computed in the resultant formulation, the stress output to the binary databases for the resultant elements are zero.

This material law is based on standard composite lay-up theory. The implementation, [See Jones 1975], allows the calculation of the force, N , and moment, M , stress resultants from:

$$\begin{Bmatrix} N_x \\ N_y \\ N_{xy} \end{Bmatrix} = \begin{bmatrix} A_{11} & A_{12} & A_{16} \\ A_{21} & A_{22} & A_{26} \\ A_{16} & A_{26} & A_{66} \end{bmatrix} \begin{Bmatrix} \epsilon_x^0 \\ \epsilon_y^0 \\ \epsilon_z^0 \end{Bmatrix} + \begin{bmatrix} B_{11} & B_{12} & B_{16} \\ B_{21} & B_{22} & B_{26} \\ B_{16} & B_{26} & B_{66} \end{bmatrix} \begin{Bmatrix} \kappa_x \\ \kappa_y \\ \kappa_{xy} \end{Bmatrix}$$

$$\begin{Bmatrix} M_x \\ M_y \\ M_{xy} \end{Bmatrix} = \begin{bmatrix} B_{11} & B_{12} & B_{16} \\ B_{21} & B_{22} & B_{26} \\ B_{16} & B_{26} & B_{66} \end{bmatrix} \begin{Bmatrix} \epsilon_x^0 \\ \epsilon_y^0 \\ \epsilon_z^0 \end{Bmatrix} + \begin{bmatrix} D_{11} & D_{12} & D_{16} \\ D_{21} & D_{22} & D_{26} \\ D_{16} & D_{26} & D_{66} \end{bmatrix} \begin{Bmatrix} \kappa_x \\ \kappa_y \\ \kappa_{xy} \end{Bmatrix}$$

where A_{ij} is the extensional stiffness, D_{ij} is the bending stiffness, and B_{ij} is the coupling stiffness, which is a null matrix for symmetric lay-ups. The mid-surface strains and curvatures are denoted by ϵ_{ij}^0 and κ_{ij} , respectively. Since these stiffness matrices are symmetric, 18 terms are needed per shell element in addition to the shell resultants, which are integrated in time. This is considerably less storage than would typically be required with through thickness integration which requires a minimum of eight history variables per integration point, e.g., if 100 layers are used 800 history variables would be stored. Not only is memory much less for this model, but the CPU time required is also considerably reduced.

***MAT_COMPOSITE_MATRIX**

This material is used for modeling the elastic responses of composites where pre-integration, which is done outside of LS-DYNA unlike the lay-up option above, is used to compute the extensional, bending, and coupling stiffness coefficients for use with the Belytschko-Tsay and the assumed strain resultant shell formulations. Since the stresses are not computed in the resultant formulation, the stresses output to the binary databases for the resultant elements are zero.

The calculation of the force, N_{ij} , and moment, M_{ij} , stress resultants is given in terms of the membrane strains, ϵ_i^0 , and shell curvatures, κ_i , as:

$$\begin{Bmatrix} N_x \\ N_y \\ N_{xy} \\ M_x \\ M_y \\ M_{xy} \end{Bmatrix} = \begin{bmatrix} C_{11} & C_{12} & C_{13} & C_{14} & C_{15} & C_{16} \\ C_{21} & C_{22} & C_{23} & C_{24} & C_{25} & C_{26} \\ C_{31} & C_{32} & C_{33} & C_{34} & C_{35} & C_{36} \\ C_{41} & C_{42} & C_{43} & C_{44} & C_{45} & C_{46} \\ C_{51} & C_{52} & C_{53} & C_{54} & C_{55} & C_{56} \\ C_{61} & C_{62} & C_{63} & C_{64} & C_{65} & C_{66} \end{bmatrix} \begin{Bmatrix} \epsilon_x^0 \\ \epsilon_y^0 \\ \epsilon_z^0 \\ \kappa_x \\ \kappa_y \\ \kappa_{xy} \end{Bmatrix}$$

where $C_{ij} = C_{ji}$. In this model this symmetric matrix is transformed into the element local system and the coefficients are stored as element history variables.

In a variation of this model, *MAT_COMPOSITE_DIRECT, the resultants are already assumed to be given in the element local system which reduces the storage since the 21 coefficients are not stored as history variables as part of the element data. The shell thickness is built into the coefficient matrix and, consequently, within the part ID, which references this material ID, the thickness must be uniform.

***MAT_MODIFIED_FORCE_LIMITED**

This material for the Belytschko-Schwer resultant beam is an extension of material 29. In addition to the original plastic hinge and collapse mechanisms of material 29, yield moments may now be defined as a function of axial force. After a hinge forms, the moment transmitted by the hinge is limited by a moment-plastic rotation relationship.

Plastic hinges form at the ends of the beam when the moment reaches the plastic moment. The plastic moment versus rotation relationship is specified by the user in the form of a load curve and scale factor. The points of the load curve are (plastic rotation in radians, plastic moment). Both quantities should be positive for all points, with the first point being (zero, initial plastic moment). Within this constraint any form of characteristic may be used, including flat or falling curves. Different load curves and scale factors may be specified at each node and about each of the local s and t axes.

Axial collapse occurs when the compressive axial load reaches the collapse load. Collapse load versus collapse deflection is specified in the form of a load curve. The points of the load curve are either (true strain, collapse force) or (change in length, collapse force). Both quantities should be entered as positive for all points, and will be interpreted as compressive. The first point should be (zero, initial collapse load).

The collapse load may vary with end moment as well as with deflections. In this case several load-deflection curves are defined, each corresponding to a different end moment. Each load curve should have the same number of points and the same deflection values. The end moment is defined as the average of the absolute moments at each end of the beam and is always positive.

Stiffness-proportional damping may be added using the damping factor λ . This is defined as follows:

$$\lambda = \frac{2\xi}{\omega}$$

where ξ is the damping factor at the reference frequency ω (in radians per second). For example if 1% damping at 2Hz is required

$$\lambda = \frac{2 \cdot 0.01}{2\pi \cdot 2} = 0.001592$$

If damping is used, a small time step may be required. LS-DYNA does not check this so to avoid instability it may be necessary to control the time step via a load curve. As a guide, the time step required for any given element is multiplied by $0.3L/c\lambda$ when damping is present (L = element length, c = sound speed).

Plastic hinges can form due to the combined action of moments about the three axes. This facility is activated only when yield moments are defined in the material input. A hinge forms when the following condition is first satisfied.

$$\left(\frac{M_r}{M_{ryield}} \right)^2 + \left(\frac{M_s}{M_{syield}} \right)^2 + \left(\frac{M_t}{M_{tyield}} \right)^2 \geq 1$$

where,

M_r, M_s, M_t = current moment

$M_{ryield}, M_{syield}, M_{tyield}$ = yield moments

Note that scale factors for hinge behavior defined in the input will also be applied to the yield moments: for example, M_{syield} in the above formula is given by the input yield moment about the local axis times the input scale factor for the local s axis. For strain-softening characteristics, the yield moment should generally be set equal to the initial peak of the moment-rotation load curve.

On forming a hinge, upper limit moments are set. These are given by

$$M_{rupper} = \text{MAX} \left(M_r, \frac{M_{ryield}}{2} \right)$$

and similar for M_s and M_t .

Thereafter the plastic moments will be given by

$$M_{rp} = \min (M_{rupper}, M_{rcurve}) \text{ and similar for s and t}$$

where

M_{rp} = current plastic moment

M_{rcurve} = moment taken from load curve at the current rotation scaled according to the scale factor.

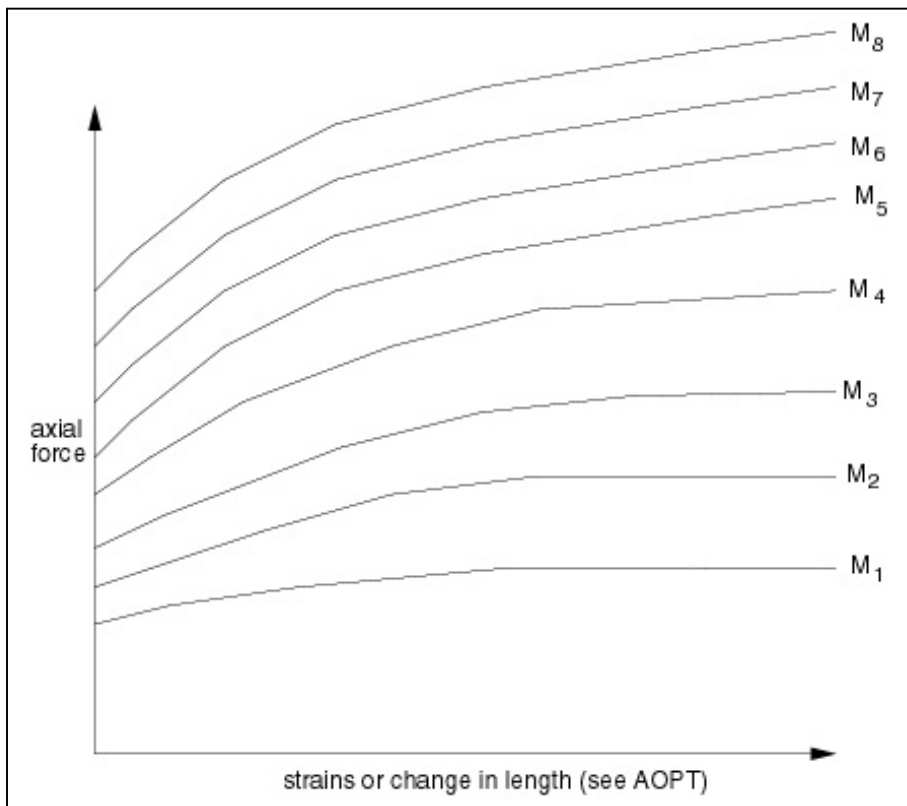
The effect of this is to provide an upper limit to the moment that can be generated; it represents the softening effect of local buckling at a hinge site. Thus if a member is bent about its local s-axis it will then be weaker in torsion and about its local t-axis. For moments-softening curves, the effect is to trim off the initial peak (although if the curves subsequently harden, the final hardening will also be trimmed off).

It is not possible to make the plastic moment vary with the current axial load, but it is possible to make hinge formation a function of axial load and subsequent plastic moment a function of the moment at the time the hinge formed. This is discussed in the next section.

In addition to the moment interaction equation, plastic hinges can form independently for the s-axis and t-axis at each end of the beam and also for the torsional axis. A plastic hinge is assumed to form if any component of the current moment exceeds the yield moment as defined by the yield moment vs. axial force curves. If any of the 5 curves are omitted, a hinge will not form for that component. The curves can be defined for both compressive and tensile axial forces. If the axial force falls outside the range of the curve, the first or last point in the curve will be used. A hinge forming for one component of moment does not effect the other components.

Upon forming a hinge, the magnitude of that component of moment will not be permitted to exceed the current plastic moment. The current plastic moment is obtained by interpolating between the plastic moment vs. plastic rotation. Curves may be input for up to 8 hinge moments, where the hinge moment is defined as the yield moment at the time that the hinge formed. Curves must be input in order of increasing hinge moment and each curve should have the same plastic rotation values. The first or last curve will be used if the hinge moment falls outside the range of the curves.

A hinge will form if either the independent yield moment is exceeded or if the moment interaction equation is satisfied. If both are true, the plastic moment will be set to the minimum of the interpolated value and M_{rp} .



The force magnitude is limited by the applied end moment. For an intermediate value of the end moment LS-DYNA interpolates between the curves to determine the allowable force value.

REFERENCES

- Broadhouse, B.J., "The Winfrith Concrete Model in LS-DYNA3D," Report: SPD/D(95)363, Structural Performance Department, AEA Technology, Winfrith Technology Centre, U.K. (1995).
- Jones, R.M., Mechanics of Composite Materials, Hemisphere Publishing Corporation, New York, (1975).
- Puso, M.A. and Weiss, J.A., "Finite Element Implementation of Anisotropic Quasilinear Viscoelasticity Using a Discrete Spectrum Approximation", ASME J. Biomech. Engng., 120, 62-70 (1998).
- Weiss, J.A., Maker, B.N. and Govindjee, S., "Finite Element Implementation of Incompressible, Transversely Isotropic Hyperelasticity", Comp. Meth. Appl. Mech. Eng., 135, 107-128 (1996).
- Whirley, R. G., and G.A. Henshall, "Creep Deformation Structural Analysis Using An Efficient Numerical Algorithm," IJNME, Vol. 35, pp. 1427-1442, (1992).

IMPROVEMENTS IN THE KEYWORD READER

***SET_..._GENERAL**

This command is now available as an easy method for defining sets. For example NODE sets can be defined by specifying options under GENERAL. i.e, ***SET_NODE_GENERAL** by using the following keywords that apply to node sets:

- ALL, all nodes
- NODE, given nodes
- DNODE, delete given nodes from set
- PART, include all nodes from listed part ID
- DPART, delete all nodes from listed part Ids
- BOX, include all nodes in listed box IDs
- DBOX, delete all nodes in listed box Ids

An arbitrary number of options can be used in a given set definition. These options are executed in the order that they are defined.

***INCLUDE_TRANSFORM**

This command is available to transform data within an INCLUDE file. This feature makes it very simple to take an existing model and reuse it in another analysis. Some key attributes of this feature are:

Identification numbers within and INCLUDE file can be offset including:

- Nodes and elements
- Parts, materials, sets, load curves, etc.

To change computational units and physical location of the model, input data can be scaled and transformed:

- Mass, temperatures, time, length, etc.

The transformed keyword data is saved written into a file: *dyna.inc* which can be used later with ***INCLUDE** keyword to avoid repeating the translation process.

***INCLUDE_STAMPED_PART**

This command provides a simple means of coupling stamping with the crash simulations. In this option the thickness and plastic strain distributions in crash models are initialized automatically. Although the residual stresses after springback from the stamping operation could easily be included, it is not, since the initial stress distribution in the vehicle is affected by the assembly process and cannot be reasonably estimated. In the current implementation an arbitrary number of parts can be initialized by including multiple *dynain* output files as INCLUDE files from the stamping analysis. The *dynain* file is created at the end of the springback calculation. To ensure ease of use, node and element Ids are not assumed to be unique between the crash model and the stamping models. Between the stamped part and the crash part:

- Arbitrary meshes are assumed
- Element formulations can change
- Three nodes on each part are used for orientation
- Number of in plane integration points can change

- Number of through thickness points can change

Full interpolation is used in the remapping process to ensure accurate values for the initialized variables.

NOVEMBER'S IMPLICIT FAQ

By Dr. Bradley Maker

(Implicit FAQ will be printed monthly)

Question:

How can I perform a metal forming simulation followed by trimming and springback?

Answer:

Since this simulation involves trimming, it can not be performed in a single run. You must first solve the forming problem, and use *INTERFACE_SPRINGBACK_DYNA3D to create a "dynain" file. Then a second simulation can be used to do the trimming and springback. This second simulation will trim at the start of the job, and can be entirely implicit thereafter (for springback).

Use *ELEMENT_TRIM and *DEFINE_CURVE_TRIM to perform the trimming at the start of the second simulation. (You can set the termination time to zero if you would like to view the trim results without proceeding to the springback simulation.)

Question:

In my implicit simulation, when I switched to linear equation solver formulations to LSOLVR=10 I got a floating point exception error and the job died immediately. Why?

Answer:

The iterative equation solvers are much less forgiving when you give them a singular matrix to invert. Our default solver has the best chance of continuing to run in spite of stiffness matrix problems.

PROVING ITS WORTH

(c) Copyright, 2000, Bruce Morse & Arthur Tang,
Engineering Technology Associates Inc. USA
Tire Technology International, June 2000 edition
published by UK & International Press - reprinted with permission

Article Excerpts: To read the full article visit www.feapublications.com

The driverless test vehicle starts from a resting position, accelerates to 30km/h, then travels for several torturous seconds over a rough cobblestone surface. During the event, the tires deform and bounce, striking the stones over and over; the suspension bends to absorb the violent weight of the vehicle body as it races forward and the joints between these components are forced to absorb every stress the road creates...This data will ultimately be used to determine the durability of the vehicle's components, how the vehicle handles on this type of road surface, its maneuverability and its fatigue life...it is actually a description of a virtual proving ground (VPG) test being performed on a supercomputer with a finite element model...

VPG TECHNOLOGY: ...VPG technology could potentially reduce the number of prototypes, drastically shorten the design cycle, and reduce product development risk and cost...

Technology Problems: Until recently, the cost of CPU power required for a full-vehicle proving ground simulation outweighed the benefits...The key to making the technology work was the development of an efficient, effective tire model...

FEA tire model: Engineering Technology Associates, Inc. has developed such a tire for use in a proprietary software known as eta/VPG - VPG standing for virtual proving ground. This software package, driven by the explicit non-linear dynamic finite element solver LS-DYNA, incorporates a finite element tire model for the transmission of forces generated from the interaction between the road surface to chassis/suspension and the vehicle body...

CONCLUSION: The primary use of this tire model has been the simulation of vehicle proving ground events....To date the VPG program has been used to evaluate a number of passenger vehicles, including a sport utility vehicle, a subcompact car, a luxury sedan, a minivan and several non-production prototypes...

Engineering Technology Associates (ETA)

www.eta.com

FEA Information Web Site News

By: Marsha Victory

FEA Information's Web Site Additions:

FEA Information News: In October, 2000, we e-mailed our first issue.

www.linuxforpc.com: We have officially opened our application site, Linux For PC.

www.ls-dyna.com: We have added the LS-DYNA application Manufacturing.

We started the application information with a clothing project on bra analysis by the consulting engineers, Ove Arup & Partners' Advanced Technology Group who used dynamic non-linear element techniques to analyze the bra's structural performance. The AVI for this project is #61.

Additionally on this site, under the application area Metal Forming, we added to our FAQ #9-11.

AVI Library and Heat Transfer Analysis site: AVI 72 was added. The welding example shows LS-DYNA applied to a coupled thermal-structural analysis of a welding process.

Massively Parallel Computers: Information was added to this site

November's Showcased Resource Site:

An informative site owned and operated by Boerries Burkhardt:

Hydroforming.net. To quote directly from his site: "Welcome to the hydroforming.net. The number one source for the hydroforming technology. Hydroforming.net gives you the platform to communicate with the right people."

www.hydroforming.net

Personal Message From FEA Information Co.:

I would like to take this opportunity to thank all of the readers of the feainformation web sites for sending me their opinions, criticisms, ideas, and corrections. Without this kind of cooperative and supportive input, I could not continue to build the sites and this newsletter into an effective information source for the engineering community. Please feel free to continue to send me your e-mail comments and suggestions.

Sincerely,

**Marsha Victory: mv@feainformation.com
President, FEA Information Co.**

Conference Proceeding Publications **by: Denette Trowbridge**

Showcased on the FEA Information news page for the month of October were the following publications. If you would like a copy e-mailed to you in pdf format contact me at: dt@feainformation.com

#D3-3-c

Virtual Proving Ground - A CAE Tool for Automotive Durability and NVH Applications
Arthur Tang, Nasser Tamini, and David Yang (ETA)

#F5-1-c

Simulation of Structural Latches in and Automotive Seat System Using LS-DYNA
Tuhin Halder (Lear Corp.)

#C2-2-c

Accurate and Detailed LS-DYNA FE Models of the US- and Eruosid: A Review of the German FAT Project
Ulrich Franz, Oliver Graf (CAD-FEM GmbH); Andreas Hirth, Matthias Walz (DaimlerChrysler, AG)

#I11-2-c

Global and Local Coupling Analysis for Small Components in Drop Simulation
Jason Wu (Motorola)

Sponsors of our November FEA Information Global News:

Livermore Software Technology Corporation (LSTC)

Develops and supports the LS-DYNA family of analysis tools, including LS-DYNA, a highly advanced multi-physics simulation code capable of providing accurate and rapid solutions to structural simulation problems of any size or complexity. LSTC is headquartered in Livermore, CA, USA.

www.lstc.com

Engineering Technology Associates (ETA)

ETA is an engineering consulting company specializing in automotive Computer Aided Engineering (CAE). ETA provides services, software, training and technology to its customers worldwide. ETA is headquartered in Troy, Michigan, USA.

www.eta.com

OASYS, LTD.

Markets engineering software products developed to the exacting standards of Ove Arup & Partners. Ove Arup is a global organization of consulting engineers, planners and project managers. Arup headquarters are located in the UK.

www.arup.com/dyna